J Solid State Electrochem (2012) 16:1187–1191
DOI 10.1007/s10008-011-1499-0

ORIGINAL PAPER

Oxygen non-stoichiometry and defect equlibria in $CaMnO_{3-\delta}$

Ekaterina I. Goldyreva · Ilya A. Leonidov · Mikhail V. Patrakeev · Victor L. Kozhevnikov

Received: 6 June 2011 / Revised: 29 June 2011 / Accepted: 30 June 2011 / Published online: 29 July 2011

Abstract A defect equilibrium model is suggested for $CaMnO_{3-\delta}$ based on oxygen non-stoichiometry and conductivity data. The model includes reactions of oxygen exchange and thermal excitation of electrons. The respective equilibrium constants, enthalpies and entropies for the reactions entering the model are obtained from the fitting of the calculated and experimental data for oxygen non-stoichiometry. The energy parameters obtained from the model and variations in the concentration of manganese species enable explanation of temperature and oxygen pressure dependencies of thermopower and conductivity within frameworks of a small polaron type model.

Keywords Calcium manganite · Perovskite · Oxygen non-stoichiometry · Defect chemistry · Equilibrium constants

Introduction

High concentration of electron and ion defects in 3*d* non-stoichiometric perovskites $ABO_{3-\delta}$ largely affect properties of these compounds, which are important in a number of applications such as solid state fuel cells, gas sensors, membrane reactors, etc. [1–4]. Studies of non-stoichiometry δ as a function of temperature T and oxygen pressure p_{O_2} enable the determination of equilibrium constants and defect concentrations [5–9]. Generally, defect formation is related with reactions of oxidation

$$\tfrac{1}{2}O_2(g) + V_O^{\bullet\bullet} + 2B_B^{'} = O_O^{\times} + 2B_B^{\times} \quad (1)$$

and thermal excitation of electrons in conduction band

$$0 = e' + h^{\bullet} \quad (2)$$

Here, Kröger–Vink notations are used [10]. When the enthalpy ΔH_D° for reaction 2 is large enough, electrons and holes are strongly localized. Typical oxides with localized electron defects are ferrites $La_{1-x}Sr_xFeO_{3-\delta}$ and their doped derivatives where ΔH_D°, varies within 1.5–2 eV [5, 6, 11–14]. Manganites $La_{1-x}Sr_xMnO_{3-\delta}$ give another example where the approximation of localized electron defects $Mn_{Mn}^{'}$ and $Mn_{Mn}^{\bullet}$ results in sufficiently good property description [7]. It is surprising therefore that contradictions still exist concerning defect concentrations and formation energies in calcium manganite $CaMnO_{3-\delta}$ though ample data on oxygen non-stoichiometry and electric properties are available in literature [15–21]. In this work, we have attempted to consider defect equilibrium in $CaMnO_{3-\delta}$ based on our earlier non-stoichiometry data obtained by a coulometric titration technique [17]. It is shown that suggested defect model enables one to explain changes in non-stoichiometry and conductivity with variations of temperature and oxygen pressure.

Experimental

The calcium manganite was obtained as described elsewhere [17]. The X-ray diffraction showed single phase $CaMnO_{3-\delta}$ with the orthorhombic lattice parameters a= 5.281(1), b=7.453(1) and c=5.266(1)Å. Rectangular bars 2×2×15 mm cut from the sintered pellets were used for

E. I. Goldyreva · I. A. Leonidov (✉) · M. V. Patrakeev · V. L. Kozhevnikov
Institute of Solid State Chemistry, Ural Branch of Russian Academy of Sciences,
91 Pervomaiskaya Str.,
Ekaterinburg, Russian Federation
e-mail: leonidov@imp.uran.ru

four-probe d.c. conductivity (σ) measurements. Current leads of platinum wire (0.3 mm) were tightly wound to the sample at 14-mm spacing while the spacing between the potential probes was 10 mm. The measurements were carried out in an electrochemical cell utilizing oxygen sensing and pumping properties of cubically stabilized zirconia oxygen electrolyte as described in [22]. The electrical parameters were measured with a high-precision SOLARTRON 7081 voltmeter. Experimental data points were collected only after equilibrium had been achieved between the sample and ambient oxygen gas, i.e., when changes in the logarithm of the conductivity did not exceed 0.01% per minute. The measurements were carried out in isothermal runs. The measurements were halted upon the achievement of the desirable low-pressure limit. Then, the oxygen pressure was increased to the starting upper limit where measurements were repeated in order to confirm reversibility of the experiment; thereupon temperature was changed thus enabling the next measuring cycle. The $p_{O_2}-T-\delta$ diagram obtained by a coulometric titration technique in [17] was used in order to obtain defect equilibrium constants.

Results and discussion

Defect equilibrium The forbidden band gap E_g is 0.7 eV according to electron band structure calculations for orthorhombic $CaMnO_{3-\delta}$ [23]. The evaluation of the intrinsic concentration of charge carries from $n=\sqrt{N_C N_V}\exp(-E_g/2kT)$, where $N_C \sim N_V \sim 1$ designate effective density of states per formula unit in conduction and valence bands, respectively, results in n=0.02–0.03 at 1000–1200 K. On the other hand, the oxygen loss δ at the same temperatures

$$CaMnO_3 \leftrightarrow CaMnO_{3-\delta} + \delta/2O_2(g) \tag{3}$$

may achieve about 0.03 [16, 17]. The concentration of charge carriers that appear in response to the oxygen loss can be estimated as $n=2\delta\sim0.06$. Therefore, the intrinsic electron-hole disordering and oxygen loss reactions may provide comparable contributions to the total concentration of charge carriers and should be considered simultaneously in defect structure analysis. The equilibrium 1 for the case of $CaMnO_{3-\delta}$ can be presented as

$$\tfrac{1}{2}O_2(g) + V_O^{\bullet\bullet} + 2Mn_{Mn}^{'} = O_O^{\times} + 2Mn_{Mn}^{\times}, \tag{4}$$

Notice also that thermal excitation of charge carriers (Eq. 2) is related with the transition of electrons from the half-filled t_{2g} to the empty e_g band of Mn^{4+} ions, so that all three charged states, Mn^{3+} ($Mn_{Mn}^{'}$), Mn^{4+} ($Mn_{Mn}^{\times}$) and Mn^{5+} ($Mn_{Mn}^{\bullet}$), occur in equilibrium, and reaction 2 can be presented in terms of equilibrium manganese species as

$$2Mn_{Mn}^{\times} = Mn_{Mn}^{'} + Mn_{Mn}^{\bullet} \tag{5}$$

This reaction may help to understand quite noticeable electron conductivity ~6 S/cm at 700 °C when oxygen non-stoichiometry δ in $CaMnO_{3-\delta}$ is virtually zero [17]. As to Mn^{5+} ions, their presence is known in manganese oxides, e.g., $Ba_3Mn_2O_8$ [24, 25]. Another example is layered perovskite $Sr_3ScMnO_{6.5\pm\delta}$ where intrinsic electron-hole equilibrium takes place near 10^{-5}–10^{-3} atm at 750–950 °C. In these conditions, δ=0 and all manganese ions are in 4+ oxidation state. The formation of Mn^{5+} ions in $Sr_3ScMnO_{6.5\pm\delta}$ at larger pressure values is evidenced by the p-type conductivity [26].

As an alternative to Eq. 5, the intrinsic electron-hole disordering in $CaMnO_{3-\delta}$ can be presented as

$$Mn_{Mn}^{\times} + O_O^{\times} = Mn_{Mn}^{'} + O_O^{\bullet} \tag{6}$$

with holes localized on oxygen ions. However, formation at high temperatures of oxygen ions with positive effective charge ($O_O^{\bullet}=^{\circ}O^{-}$) does not seem probable because 2p(O) levels are located at lower energy than 3d(Mn) levels [27]. Therefore, everywhere below the holes are regarded as associated with manganese ions.

Equilibrium constants The equilibrium constants for reactions 4 and 5 can be presented as

$$K_{Ox} = \frac{[O_O^{\times}][Mn_{Mn}^{\times}]^2}{p_{O_2}^{1/2}[V_O^{\bullet\bullet}][Mn_{Mn}^{'}]^2} \tag{7}$$

$$K_D = \frac{[Mn_{Mn}^{'}][Mn_{Mn}^{\bullet}]}{[Mn_{Mn}^{\times}]^2} \tag{8}$$

Considering defect concentrations per formula unit, $CaMn_a^{4+}Mn_n^{3+}Mn_p^{5+}O_{3-\delta}$, the site balance and electroneutrality requirements can be written as

$$a + n + p = 1 \tag{9}$$

$$n = p + 2\delta \tag{10}$$

Combining Eqs. 9 and 10 with the respective expression for the equilibrium constant

$$K_D = \frac{np}{a^2}, \tag{11}$$

variables a, n and p can be found as

$$p = \frac{\delta + 2K_D - 4\delta K_D - \sqrt{K_D - 4\delta^2 K_D + \delta^2}}{4K_D - 1} \quad (12)$$

$$n = 2\delta + \frac{\delta + 2K_D - 4\delta K_D - \sqrt{K_D - 4\delta^2 K_D + \delta^2}}{4K_D - 1} \quad (13)$$

$$a = 1 - 2\delta - \frac{2\left(\delta + 2K_D - 4\delta K_D - \sqrt{K_D - 4\delta^2 K_D + \delta^2}\right)}{4K_D - 1} \quad (14)$$

From Eq. 7, we obtain the relationship between δ and p_{O_2}

$$p_{O_2}^{1/2} = \frac{(3-\delta)a^2}{K_{Ox}\delta n^2}, \quad (15)$$

where n and a are to be taken from Eqs. 13 and 14, respectively. The equilibrium constants K_{Ox} и K_D can be obtained from the fitting of the calculated plots $(3-\delta)$ vs. $\log p_{O_2}$ to experimental data. The model calculations and experimental results demonstrate a satisfactory agreement as can be seen in Fig. 1.

The obtained dependencies for log K_{Ox} and log K_D from inverse temperature are straight lines, Fig. 2. Hence, the known interrelation of the equilibrium constant K_j with the standard enthalpy ΔH_j° and entropy ΔS_j° of the respective reaction

$$-RT \ln K_j = \Delta H_j^\circ - T\Delta S_j^\circ \quad (16)$$

can be used in order to determine ΔH_{Ox}°, ΔS_{Ox}° and ΔH_D°, ΔS_D° for reactions 4 and 5. The results are shown in Table 1.

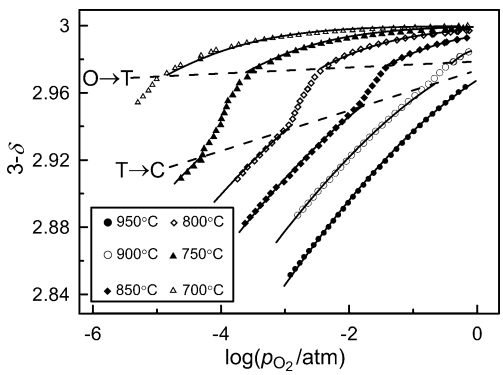

Fig. 1 Isothermal plots of oxygen content vs. oxygen partial pressure. *Solid lines* show calculation results according to Eq. 15. *Dotted lines* separate cubic (C), tetragonal (T) and orthorhombic (O) structural modifications

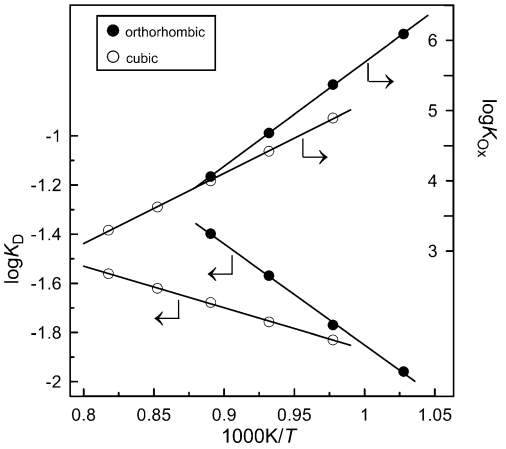

Fig. 2 Logarithmic dependencies of equilibrium constants from inverse temperature for orthorhombic and cubic modifications of $CaMnO_{3-\delta}$

As expected, the enthalpy and entropy of the reactions both depend on the structural state of $CaMnO_{3-\delta}$. Note also that near equality is expected of ΔH_{Ox}° and oxygen partial molar enthalpy $\Delta\overline{H}_O$ in oxides where electrical neutrality condition is $n=2\delta$ [28]. Considering $\Delta H_{Ox}^\circ = -190$ kJ mol^{-1} obtained in this study and experimental result $\Delta\overline{H}_O = -164$ kJ mol^{-1} in [18], one can ascertain that this condition is indeed approximately satisfied in the cubic $CaMnO_{3-\delta}$ phase. Another confirmation of the consistency of the suggested defect model can be seen from favorable comparison of calculated values, 78 kJ/mol (0.8 eV) and 33 kJ/mol (0.35 eV), for the enthalpy ΔH_D°, which is essentially equal to the band gap, with the values for the band gap, 0.7 eV and 0.46 eV, obtained in electron structure simulations for orthorhombic and cubic polymorphs of $CaMnO_{3-\delta}$, respectively [23].

Reactions 4 and 5 involve the redistribution of electric charge over manganese ions. The change in equilibrium and the accompanying transport of charge in the crystal lattice seem to be easier in the case of less deformed transport chains … Mn–O–Mn… Hence, it is not surprising to see the absolutes values for ΔH_D° and ΔH_{Ox}° smaller in the cubic phase, where the bond angle (Mn–O–Mn) is straight, while larger values for ΔH_D° and ΔH_{Ox}° reflect considerable deformation of the bond angle, (Mn–O–Mn)=158°, in the orthorhombic structure [29, 30]. This particular observation may possibly have a wider application, and absolute values

Table 1 The enthalpy and entropy values for reactions 4 and 5 in orthorhombic and cubic $CaMnO_{3-\delta}$

Structure	ΔH_{Ox}°, kJ mol^{-1}	ΔS_{Ox}°, J mol^{-1}K^{-1}	ΔH_D°, kJ mol^{-1}	ΔS_D°, J mol^{-1}K^{-1}
Orthorhombic	−286±10	−177±8	78.0±4.0	42.4±2.2
Cubic	−190±7	−92±5	33.4±1.8	−3.0±0.4

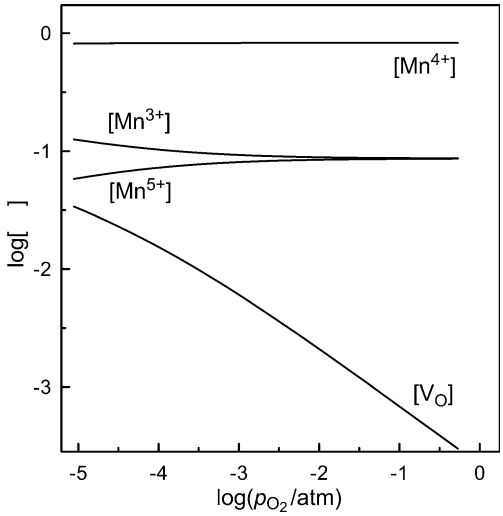

Fig. 3 Variations with the pressure of oxygen non-stoichiometry and the concentration of manganese species in $CaMnO_{3-\delta}$ at 700 °C

for defect formation enthalpies always tend to become larger with the lowering of the symmetry of the perovskite lattice. For instance, the absolute values for partial enthalpy of oxygen in orthorhombic $YBa_2Cu_3O_{7-\delta}$ are larger than in the tetragonal structure [31]. The enthalpy values $|\Delta H^{\circ}_{Ox}|$ are larger in the orthorhombic than in the less deformed rhombohedral ferrites $La_{1-x}Sr_xFeO_{3-\delta}$ [11] seem also to support this conclusion.

Concentration of manganese species Eqs. 12–15 can be used in order to calculate changes in oxygen non-stoichimetry and concentration of different manganese ions with variations of oxygen pressure and temperature. The respective results are shown for the orthorhombic phase at 700 °C in Fig. 3 and for the cubic phase at 950 °C in Fig. 4.

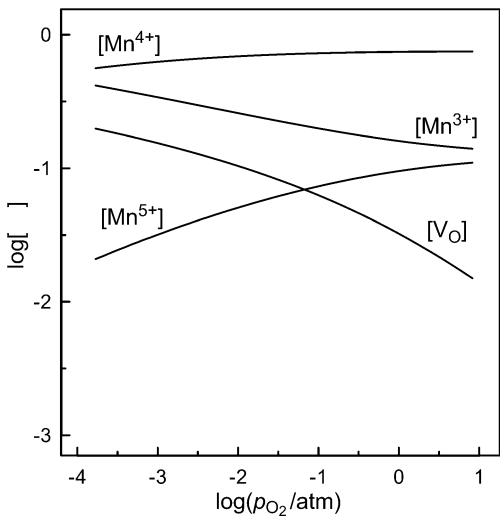

Fig. 4 Variations with the pressure of oxygen non-stoichiometry and the concentration of manganese species in $CaMnO_{3-\delta}$ at 950°C

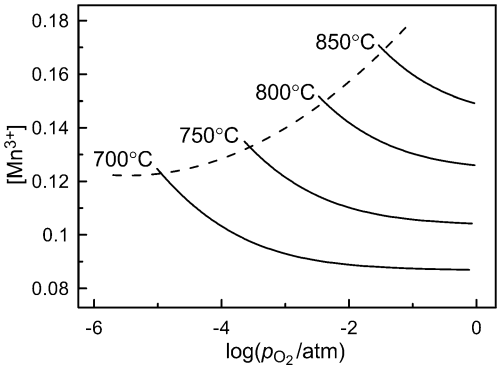

Fig. 5 Calculated isothermal variations in the concentration of Mn^{3+} ions at the changes of oxygen partial pressure. The *dotted line* shows stability border for the orthorhombic $CaMnO_{3-\delta}$

It is seen that at moderate temperatures thermal excitation of t_{2g} electrons to the empty e_g band is mainly responsible for the appearance of charge carriers. Additional evidence to reaction 5 being active at 400–700 °C, where δ is quite small [16, 17], is given by thermopower measurements. While heating in this temperature range has no significant impact upon oxygen content in $CaMnO_{3-\delta}$, the concentration increase of Mn^{3+} ions according to Eq. 5 results in the decrease of the concentration quotient in the expression for thermopower

$$S = -\frac{k}{e}\ln\left(\frac{1-[Mn^{3+}]}{[Mn^{3+}]}\right), \tag{17}$$

and in appreciable decrease of the thermopower absolute values [17].

The increase in temperature and the decrease in pressure both facilitate reaction 4. The calculated variations in the concentration of electrons with temperature and oxygen pressure are shown for the orthorhombic phase in Fig. 5. Assuming a small polaron type conduction mechanism, the conductivity in $CaMnO_{3-\delta}$ should be proportional to the product of the concentration of carriers $[Mn^{3+}]$ and

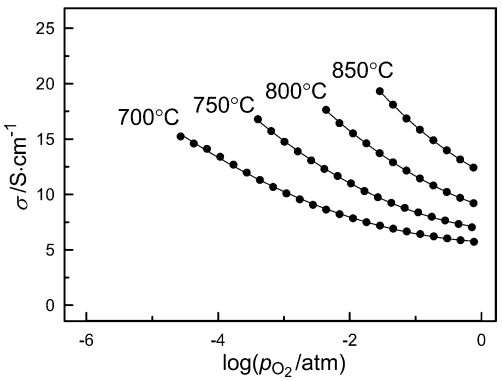

Fig. 6 Isothermal variations of electrical conductivity in orthorhombic $CaMnO_{3-\delta}$ at the changes of oxygen partial pressure

positions [Mn^{4+}] available for the hops of polarons, i.e. $\sigma \sim [Mn^{3+}][Mn^{4+}]$. Considering relatively small variations of [Mn^{4+}] in Figs. 3 and 4, the conductivity increase with the pressure decrease in Fig. 6 is mainly governed by changes in the concentration of Mn^{3+} ions (see Fig. 5). In general, heating results in the formation of Mn^{3+} ions in amount sufficient for rather high conductivity even when $\delta \approx 0$.

The data in Figs. 5 and 6 can be used in order to evaluate the mobility of electrons in $CaMnO_{3-\delta}$ according to

$$\mu = \frac{\sigma}{e \cdot n \cdot N}, \tag{18}$$

Here, e is elementary charge, n is amount of electrons per formula unit, N is amount of formula units per unit volume that can be calculated from structural data [28, 29]. The mobility calculated at 700–950 °C varies within 0.02–0.04 cm^2V^{-1} s^{-1} at changes of oxygen partial pressure. These values are consistent with the small polaron conduction mechanism.

Conclusions

The analysis of oxygen non-stoichiometry and electrical conductivity variations in $CaMnO_{3-\delta}$ with temperature and partial pressure of oxygen has shown that defect equilibrium involves oxygen exchange and thermal excitation of electrons. A satisfactory correspondence of experimental and calculated values for the non-stoichiometry parameter is achieved when electron and hole are treated as localized on manganese ions. The equilibrium constants are shown to strongly depend on crystalline structure of $CaMnO_{3-\delta}$. The absolute values for defect formation enthalpies larger in the orthorhombic than in the cubic phase are explained as a consequence of heavier distortions of crystalline lattice in the orthorhombic structure.

Acknowledgments Partial support of this work by the Russian Foundation for Basic Research under grant no. 10-03-00475a is gratefully acknowledged.

References

1. Ishihara T, Matsuda H, Takita Y (1995) Solid State Ionics 79:147–151
2. Radhakrisnan R, Virkar AV, Singhal SC (2005) J Electrochem Soc 152:A210–A218
3. Alcock CB, Doshi RC, Shen Y (1992) Solid State Ionics 51:281–289
4. Balachandran V, Dusek JT, Mieville RL, Poeppel RB, Kleefisch MS, Pei S, Kobylinski TP, Udovich CA, Bose AC (1995) Appl Catal A 133:19
5. Mizusaki J, Yoshishiro M, Yamauchi S, Fueki K (1985) J Solid State Chem 58:257–266
6. Park CY, Jacobson AJ (2005) J Electrochem Soc 152:J65–J73
7. Kuo JH, Anderson HU, Sparlin DM (1989) J Solid State Chem 83:52–60
8. Van Roosmalen JAM, Corfunke EHP (1994) J Solid State Chem 110:109–112
9. Mizusaki J, Mori N, Takai H, Yonemura Y, Minamiue H, Tagawa H, Dokiya M, Inaba H, Naraya K, Sasamoto T, Hashimoto T (2000) Solid State Ionics 129:163–177
10. Kröger FA (1964) The chemistry of imperfect crystals. North-Holland, Amsterdam
11. Mizusaki J, Yoshishiro M, Yamauchi S, Fueki K (1987) J Solid State Chem 67:1–8
12. Søgaard M, Hendriksen PV, Mogensen M (2007) J Solid State Chem 180:1489–1503
13. Yoo J, Jacobson AJ (2009) J Electrochem Soc 156:B1085–B1091
14. Markov AA, Patrakeev MV, Savinskaya OA, Nemudry AP, Leonidov IA, Leonidova ON, Kozhevnikov VL (2008) Solid State Ionics 179:99–103
15. Zeng Z, Greenblatt M, Croft M (1999) Phys Rev B 59:8784–8788
16. Rørmark L, Wiik K, Stølen S, Grande T (2002) J Mater Chem 12:1058–1067
17. Leonidova EI, Leonidov IA, Patrakeev MV, Kozhevnikov VL (2011) J Solid State Electrochem 15:1071–1075
18. Bakken E, Norby T, Stølen S (2005) Solid State Ionics 176:217–223
19. Taguchi H, Sanoda M, Nagao M (1998) J Solid State Chem 137:82–86
20. Hejtmánek J, Jirák Z, Maryško M, Martin C, Maignan A, Harvieu M, Raveau B (1999) Phys Rev B 60:14057–14065
21. Fisher B, Patlagan L, Reisner GM, Knizhnik A (2000) Phys Rev B 61:470–475
22. Patrakeev MV, Mitberg EB, Lakhtin AA, Leonidov IA, Kozhevnikov VL, Kharton VV, Avdeev M, Marques FMB (2002) J Solid State Chem 167:203–213
23. Søndenå R, Stølen S, Ravindran P, Grande T, Grande NL (2007) Phys Rev B 75:184105
24. Uchida M, Tanaka H, Bartashevich MI, Goto T (2001) J Phys Soc Jpn 70:1790–1793
25. Weller MT, Skinner SJ (1999) Acta Crystallogr Sect C: Cryst Struct Commun 55:154–156
26. Chupakhina TI, Zaytseva NA, Melkozerova MA, Gyrdasova OI, Bazuev GV, Leonidov IA, Patrakeev MV, Kozhevnikov VL (2004) Proc 7-th Intern Meeting "Order, Disorder and Properties of Oxides", Sochi, Russia:246–249
27. Kofstad P (1972) Nonstoichiometry, diffusion and electrical conductivity in binary metal oxides. Wiley, New York
28. Coey JMD, Viret M, Ranno L, Ounadjela K (1995) Phys Rev Lett 75:3910–3913
29. Poeppelmeier KR, Leonowicz ME, Scanlon JC, Longo JM, Yelon WB (1982) J Solid State Chem 45:71–79
30. Chmaissem O, Dabrowski B, Kolesnik S, Mais J, Brown DE, Kruk R, Prior P, Pyles B, Jorgensen JD (2001) Phys Rev B 64:134412
31. Yamaguchi S, Terabe K, Saito A, Yanagi S, Iguchi Y (1988) Jpn J Appl Phys 27:L179–L181